SEISMIC IMAGING AND INTERPRETIVE MODEL BUILDING IN THE COLOMBIAN ANDES

ROB VESTRUM
TBI (Thrust Belt Imaging): 2300, 645 - 7 Ave SW, Calgary, Alberta, Canada

ABSTRACT

Lateral velocity variation and dipping anisotropy in the overburden cause imaging and position problems on seismic images in thrust belt environments like the Andes. Anisotropic depth migration has the greatest potential to provide the clearest seismic image and most accurate lateral position of subsurface reflectors in thrust-belt environments.

Depth migration in thrust-belt environments like the Colombian Andes requires an interpretive approach to building a depth-migration velocity model. With low fold in the near surface, a low signal-to-noise ratio on the image gathers, and complex horizon geometries, automated velocity-model-building tools fail to produce an optimum velocity model for anisotropic depth migration. In a setting with such under-constrained velocities, we compensate for the shortcomings of our seismic data by applying geologic constraints: surface-geology maps, regional structural style, well-log depths, dip-meter data.

Data examples from the Colombian Andes and from the foothills of the Canadian Rocky Mountains show the importance of integrating as much geologic information into the model-building process. The results show improvements in reflector continuity, resolution of the seismic image, and accuracy of the lateral position of structures as compared to the prestack time migration of the same data.

INTRODUCTION

Anisotropic depth migration in thrust-belt environments has the greatest potential to provide the clearest image and most accurate lateral position of subsurface (e.g., Ball, 1995; Vestrum and Muenzer, 1997; Di Nicola-Carena, 1997; Ferguson and Margrave, 1998; Vestrum et al., 1999; Stratton, 2004).

Depth migration in thrust-belt environments like the foothills of the Canadian Rockies requires an interpretive approach to building a depth-migration velocity model (Vestrum et al., 2004). With low fold in the near surface, low signal-to-noise ratios on the image gathers, and complex horizon geometries, automated velocity-model-building tools fail to produce an optimum velocity model for TTI anisotropic depth migration. In a setting with such under-constrained velocities, we must use as many geologic constraints in the interpretation of our velocity model.

THE ANISOTROPIC IMAGING PROBLEM

Anisotropic depth migration has become common in hydrocarbon exploration in thrust-belt environments. This section describes the seismic imaging problems that anisotropic depth migration works to overcome.

The sideslip effect refers to wave motion that is perpendicular to the wavefront normal. Sideslip results in the lateral mispositioning of structures below dipping clastics on seismic images when the anisotropy is ignored in the migration algorithm. Several authors propose solutions to the lateral-position problem in terms of anisotropic depth migration that handles TTI symmetry (e.g., Ball,

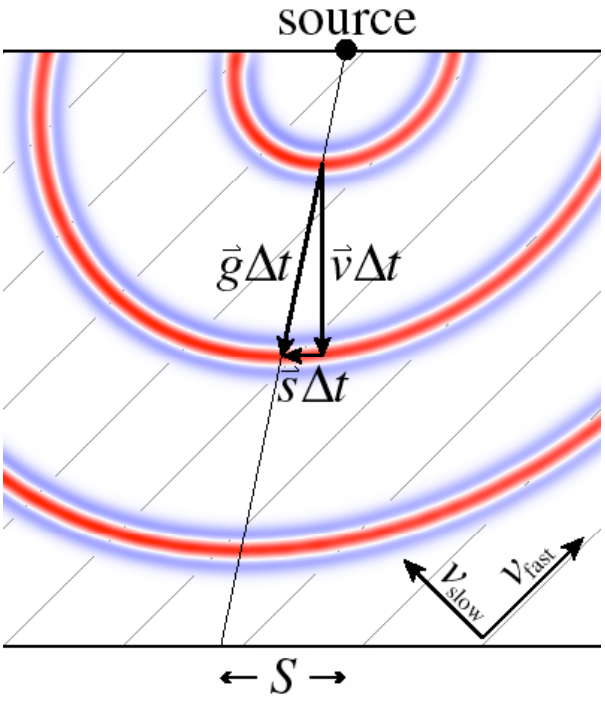

Figure 1: Waves propagating across dipping anisotropic strata separated by time Δt. The grey diagonal lines represent the 45° dip orientation. The lateral distance between the source and the zero-offset reflection point is the zero-offset sideslip distance S_0.

1995; Vestrum and Muenzer, 1997; Ferguson and Margrave, 1998; Vestrum et al., 1999). The goal of these algorithms is to improve imaging and position of seismic reflectors.

Consider imaging structures below weak transversely isotropic strata with a tilted axis of symmetry. Thomsen (1986) gives us a convenient expression for the phase velocity, *v*, as it varies with direction in terms of angle from the symmetry axis, θ, and elastic constants, ϵ and δ:

$$v(\theta) = v_0(1 + \delta \sin^2\theta\cos^2\theta + \varepsilon \sin^4\theta). \quad (1)$$

Figure 1 illustrates a propagating wavefront in a TTI medium. The phase velocity, *v*, is the velocity of the wave normal to its wavefront. The sideslip velocity, *s*, is the velocity of wave motion in the direction tangential to the wavefront (Dellinger, 1991). Vector addition of sideslip-velocity and phase-velocity vectors yields the group velocity, *g*, which is the velocity of energy transport (in a lossless medium). We obtain the equation for the sideslip velocity magnitude, *s*, by differentiating Equation 1 with respect to θ:

$$s \equiv \frac{\partial v}{\partial \theta} = v_0\left[2\delta\left(\cos^3\theta\sin\theta - \cos\theta\sin^3\theta\right) + 4\varepsilon\cos\theta\sin^3\theta\right]. \quad (2)$$

The sideslip distance, *S*, as defined by Vestrum et al. (1999), is the horizontal displacement of a reflection point from the midpoint between seismic source and receiver for a horizontal reflector below a layer of anisotropic strata with a tilted axis of symmetry. If we consider only the zero-offset sideslip distance as a function of the vertical thickness of the dipping anisotropic strata, Δ*Z*, and the magnitudes of the sideslip velocity, *s*, and phase velocity, *v*, we may define the zero-offset sideslip distance, S_0, as:

$$S_0 \equiv \frac{s}{v}\Delta Z. \quad (3)$$

This equation is valid only for the case of zero-offset distance between the source and receiver. Figure 2 illustrates how the sideslip distance changes with source-receiver offset.

Figure 2 shows minimum-traveltime raypaths for offsets ranging from zero to 2000 metres through a 1000-metre-thick TTI medium dipping 15°. The anisotropic parameters used in these tests were chosen to be ϵ = 0.12 and δ = 0.03, which are commonly used values in thrust-belt anisotropic depth migration (e.g., Vestrum, 2002; Gittins et al., 2004). Not only is the reflection point shifted laterally from the midpoint between source and receiver, but each offset images a slightly

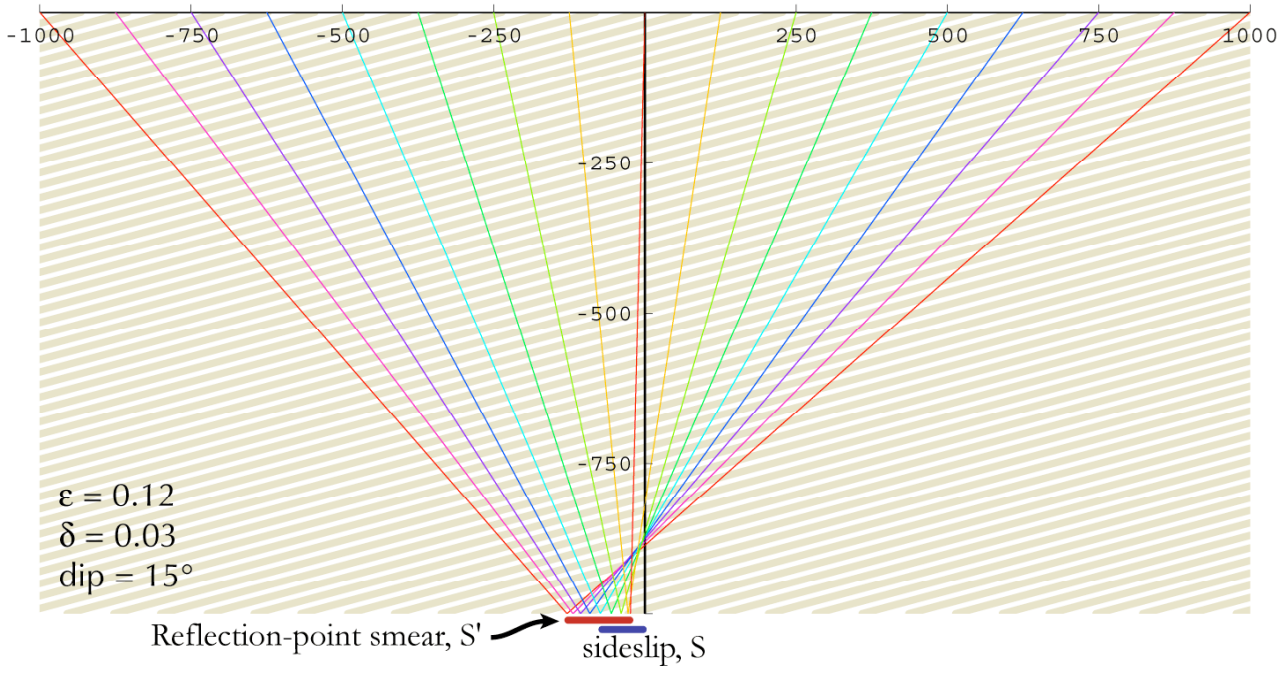

Figure 2: Lateral shift of reflection point with offset for a horizontal reflector beneath anisotropic strata dipping at 15°. Distance units are metres.

different location in the subsurface. Here the lateral shift at the far offset is much larger than the zero-offset sideslip, giving a larger average lateral shift than Equation (3) would predict. The distance from the reflection point at zero offset to the reflection point at the maximum offset is defined as the reflection-point smear, *S*' (Figure 2), because all of the traces that share this common midpoint are not imaging the same reflection point.

To see how the sideslip and smear affect seismic images, Vestrum and Fowler (2005) created numerical-model seismic data for a horizontal reflector below 2 km of dipping anisotropic strata. The various models had the same basic model geometry but for one difference: the dip of the anisotropic strata above the reflector varied from case to case. We then migrated these data ignoring anisotropy to see the residual effects of anisotropy on seismic images. Note that at the smaller overburden dip of 15° (Figure 3b), there is considerable smear on the edge of the reflector whereas at 45° (Figure 3d), there is considerable lateral-position error on the image of the structure, but less smear on the edge of the reflector.

These models illustrate the anisotropic imaging problem in simple geometry. The important points to note above are (1) anisotropy affects the lateral position of subsurface structures on seismic images and (2) imaging and position problems have a strong dependence on the dip of the anisotropic strata.

These illustrations are limited to a single dip in a homogeneous overburden, which helps us understand the wave behaviour, but if we wish to observe and correct anisotropic effects on seismic images, then we must build a velocity model that incorporates dipping anisotropic strata and perform an anisotropic depth migration.

INTERPRETIVE MODEL BUILDING

In a typical thrust-belt setting like the Andes, we observe laterally varying dip in our anisotropic

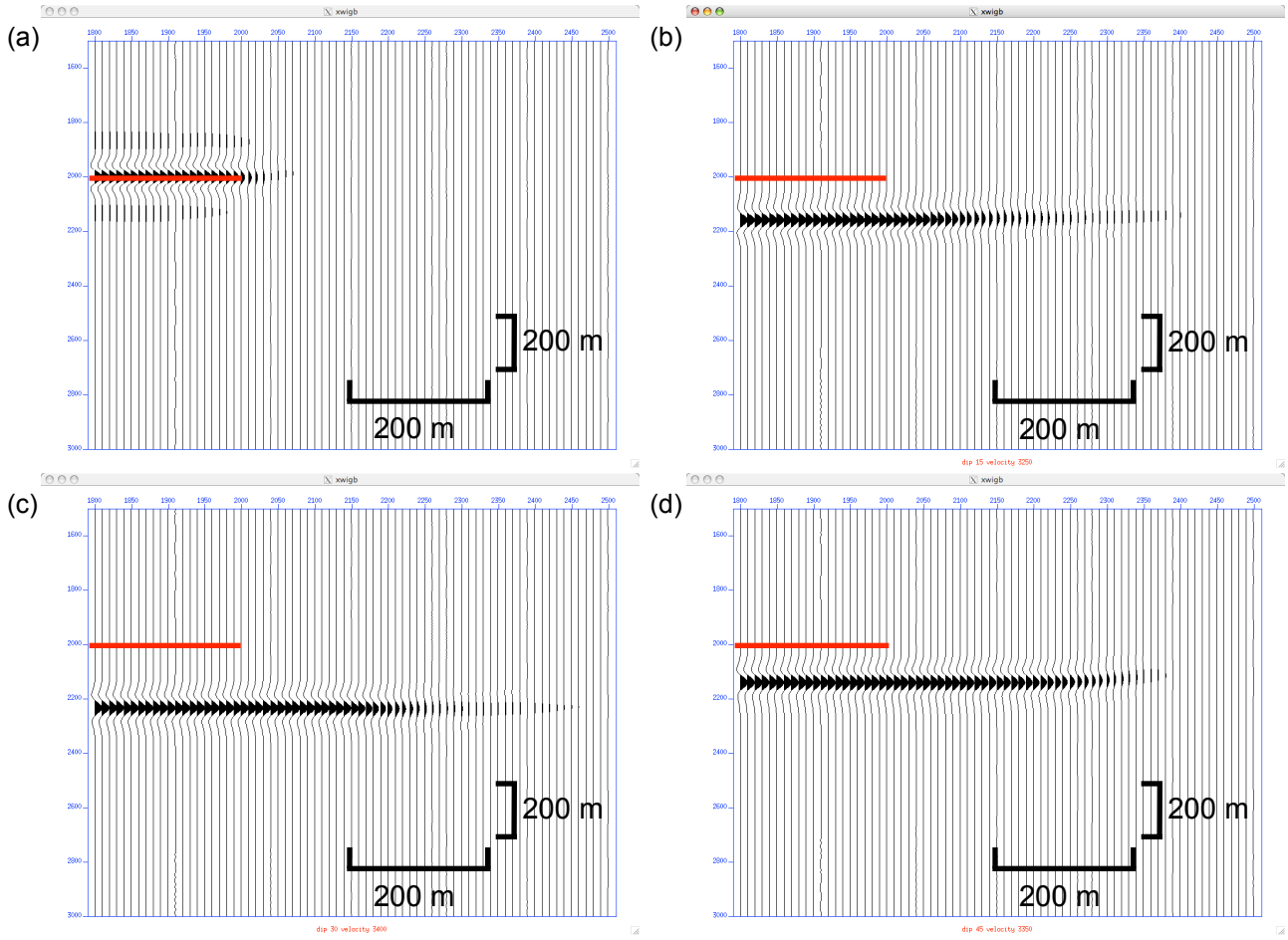

Figure 3: Depth images of physical model data. (a) anisotropic depth migration of anisotropic forward-model data shows an accurate image of the reflector. Three examples (b, c, and d) show what happens to anisotropic model data when we ignore anisotropy in seismic imaging. The dip of the anisotropy above the target is (b) 15°, (c) 30°, and (d) 45°. The red line shows the true position of the target reflector at 2 km depth.

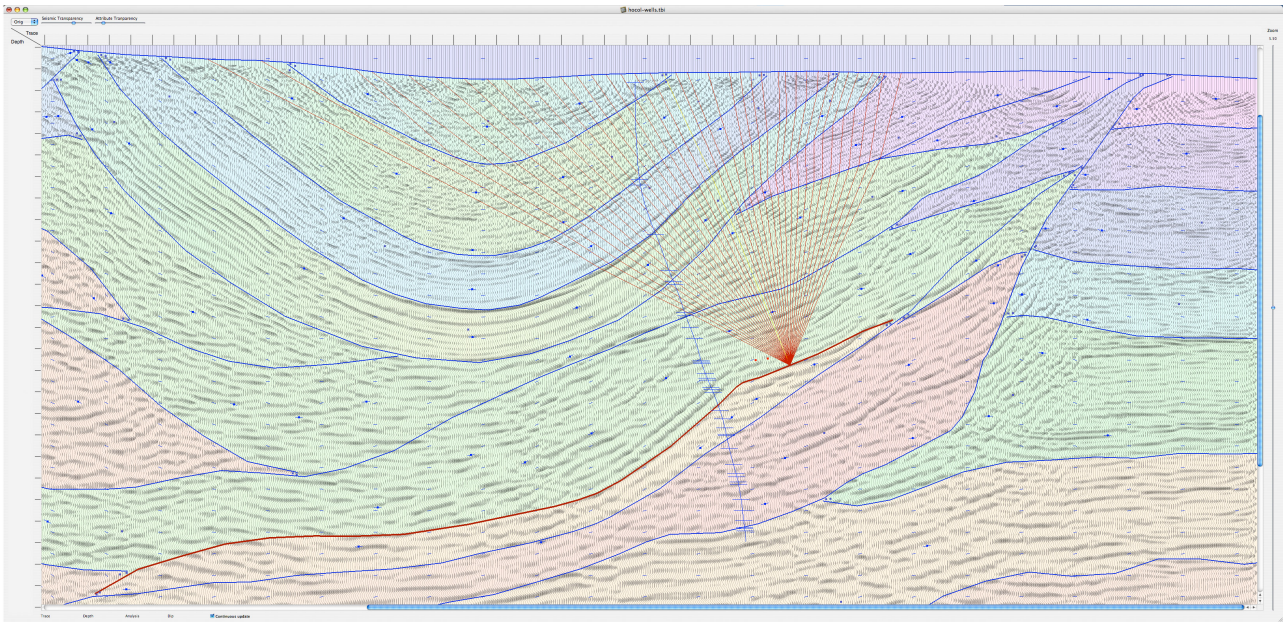

Figure 4: Interpretive model building display showing velocity cross section in colour overlaid by the depth-migrated seismic section. The rays shown in the figure are calculated for use in image-gather diagnostics.

strata. We also encounter lateral-velocity heterogeneity, which further affects the lateral position of subsurface structures. Optimum seismic imaging results from the most accurate representation of the subsurface velocity and anisotropy.

With limitations on thrust-belt seismic data of low signal-to-noise on image gathers, low fold in the near surface, and complex horizon geometries, automated or data-driven model-building tools fail to produce an optimum velocity model for TTI anisotropic depth migration. In a setting with such under-constrained velocities, we must use as many geologic constraints as possible in the interpretation of our velocity model.

Figure 5 shows an interactive model-building display with the seismic overlaid on the velocity model. For each model update, the velocity interpreters inspect the tie between the velocity horizons and the seismic reflectors. There may be improvements to the seismic image that result in a change of placement of a fault or the shape of a fold. There also may be changes in the dip of the anisotropic strata, which is also reviewed with the horizon geometry.

Figure 5 shows a close-up view of the model building display in Figure 4. The markers with the squares in the centre are manually picked dips and the tick marks without the squares are interpolated picks on a grid. The output dips are is fully interpolated onto the velocity-model grid. The reader might observe places in this display (Figure 5) where the accuracy of the model dips could be improved.

After considering the seismic image and the correlation with the velocity cross-section and the model dips, the depth imager may then select a model body for seismic velocity analysis. Raytracing through the model, as seen in Figure 4, allows the software to calculate corrections for the migrated image gathers that result from changes in the velocity of a given body.

Figure 6 shows an image-gather display with a correction applied by the raytracing calculations.

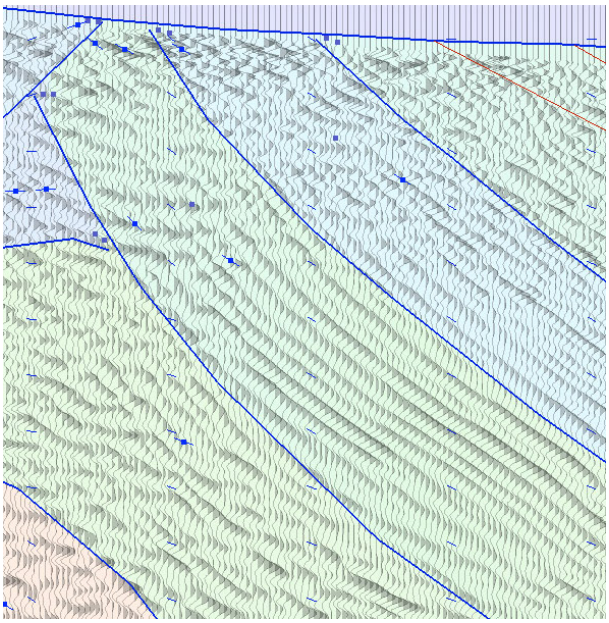

Figure 5: Close-up view of interactive model-building display in Figure 2. The blue markers are dip markers, oriented parallel to the dip of the anisotropic strata.

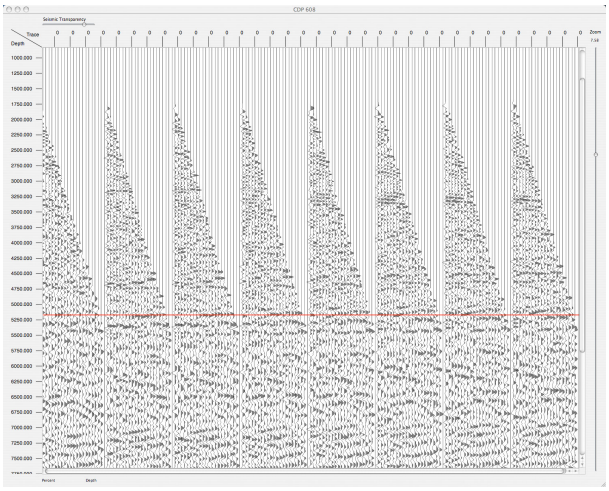

Figure 6: Image-gather diagnostics from velocity-model interpretation software. The red line shows the depth of the active horizon in Figure 4.

The depth imager may now find the velocity for the current body that best flattens the migrated image gather.

After all changes in horizon geometry and velocity are applied to the model, the resulting velocity model is input to the next iteration of anisotropic depth migration. The process continues with several velocity-building iterations until the image is optimized and any well depths match the seismic reflector depths.

The structural geologist is a key player in collecting geological constraints for the velocity model. Far more than that, the structural geologist should take a key role in the model-building process. As the model-building process progresses, there will be times when improved imaging requires a modified interpretation of key velocity boundaries and there will be times when imaging pitfalls can only be overcome with a better understanding of the geologic structures. Stratton (2004) showed how using a structural-geology constraint changed the dip interpretation in the model and resulted in a more accurate lateral position of her exploration target and improved imaging of the steep back limb.

A model-building team should consist of one or more interpreters as well as depth imagers. The key role on the interpretation side is structural interpreter. On the depth-imaging side, the key tasks include applying model updates and migration parameter testing as well as the main responsibility of co-ordinating the model interpretation. The depth imager will ensure that new model interpretations are properly applied to the velocity model and everyone involved with the project understands the sensitivities of the seismic image to the various parameter changes and the various imaging diagnostics used to guide the interpretation. The model-building team should decide together what are the realistic objectives for the project, agree on a project timeline, and decide on what criteria they will use to measure when they have reached the project objectives.

Interpretive model building can sometimes lead to a model-update dead end, where it seems that the team is making little progress toward an improved image with accurate well ties. Here is where a trial-and-error approach to a re-interpretation of the velocity model can help break out of a locally optimized model. The process works like this: build a few velocity models with alternative interpretations and run a limited output set of the migrated volume for each velocity model. Compare the resulting outputs to find the new test model that offers the best image; this model may be a starting point for a model-updating session in a new direction.

You may find that one of the trial models offers improved imaging of certain structures where another trial model offers improved imaging of structures at a different depth or position along a line. Here it is best to try to combine the two models to get the best of both images. Perhaps some lateral-variation of the velocities is required or perhaps a tweak of anisotropic parameters will help reconcile the two velocity problems. Schmid et al. (1996) diagnosed an anisotropy problem on the Husky/Talisman dataset, where structures with raypaths that cut across beds in the overburden required a different velocity to flatten the image gathers than structures with raypaths that run closer to parallel to bedding. This velocity-anisotropy diagnosis was later confirmed and the imaging problem resolved in Vestrum et al. (1999).

CONCLUSIONS

The presence of dipping clastics above exploration targets results in imaging and position problems on seismic data. Correcting for dipping anisotropy in depth imaging gives the most accurate image.

When building a velocity model for anisotropic depth migration in a complex-structure land environment like the foothills of the Andes, we need an interpretive approach to velocity-model building, using geological constraints to overcome the shortcomings in our seismic data.

Interpretive model building produces the most accurate image in foothills settings and the interpretation process provides the interpreter with

deeper understanding of the geologic setting and structural trends in the area.

REFERENCES

Alkhalifah, T., 1995, Efficient synthetic-seismogram generation in transversely isotropic, inhomogeneous media: Geophysics, Soc. of Expl. Geophys., 60, 1139-1150.

Ball, G., 1995, Estimation of anisotropy and anisotropic 3-D prestack depth migration, offshore Zaire, Geophysics 60, 1495-1513.

Dellinger, J., 1991, Anisotropic seismic wave propagation, PhD thesis, Stanford University.

Gittins, J., Vestrum, R. W., and Gillcrist, R., Overcoming thrust-belt imaging problems in South America from illumination to anisotropy, CSEG 2004 Natnl. Mtg.

Ferguson, R.J., and Margrave, G.F., 1998, Depth migration in transversely isotropic media by nonstationary phase shift, GEOTRIAD '98, Joint meeting of CSEG, CSPG, and CWLS.

Schmid, R., Link, B. and Butler, P., 1996, A comprehensive approach to depth imaging in thrust belt environments: 66th Ann. Internat. Mtg: Soc. of Expl. Geophys., 366-368.

Stratton, M.A., 2004, Impact of the effects of anisotropy in Canadian foothills exploration: A case history: 74th Annual Internat. Mtg., Soc. Expl. Geophys.

Thomsen, L., 1986, Weak elastic anisotropy: Geophysics, 51, 1954-1966.

Vestrum, R. W., 2002, 2D and 3D anisotropic depth migration case histories: 72nd Annual Internat. Mtg., Soc. Expl. Geophys.

Vestrum, R.W., and Fowler, P.J., Quantifying imaging and position problems beneath TTI media: 67th Mtg.: Eur. Assn. Geosci. Eng., E026**.**

Vestrum, R.W., and Muenzer, K., 1997, Anisotropic depth imaging below dipping shales, CSEG 1997 Natnl. Mtg.

Vestrum, R. W., **Lawton, D.C., and Schmid, R. S.**, 1999, Imaging structures below dipping TI media: Geophysics, 64, no. 4, 1239-1246.